Hindawi Publishing Corporation
International Journal of Photoenergy
Volume 2012, Article ID 638571, 7 pages
doi:10.1155/2012/638571

Research Article

Influence of the Sol-Gel pH Process and Compact Film on the Efficiency of TiO_2-Based Dye-Sensitized Solar Cells

A. O. T. Patrocinio,[1,2] A. S. El-Bachá,[1] E. B. Paniago,[3] R. M. Paniago,[4] and N. Y. Murakami Iha[1]

[1] *Laboratory of Photochemistry and Energy Conversion (USP), Instituto de Química, Universidade de São Paulo, Avenue Prof. Lineu Prestes 748, 05508-900 São Paulo, SP, Brazil*
[2] *Instituto de Química, Universidade Federal de Uberlândia 38400-902 Uberlândia, MG, Brazil*
[3] *Departamento de Qutmica, Universidade Federal de Minas Gerais 31270-010 Belo Horizonte, MG, Brazil*
[4] *Departamento de Física, Universidade Federal de Minas Gerais 31270-010 Belo Horizonte, MG, Brazil*

Correspondence should be addressed to N. Y. Murakami Iha, neydeiha@iq.usp.br

Received 2 December 2011; Revised 27 January 2012; Accepted 27 January 2012

Academic Editor: Leonardo Palmisano

The influence of pH during hydrolysis of titanium(IV) isopropoxide on the morphological and electronic properties of TiO_2 nanoparticles prepared by the sol-gel method is investigated and correlated to the photoelectrochemical parameters of dye-sensitized solar cells (DSCs) based on TiO_2 films. Nanoparticles prepared under acid pH exhibit smaller particle size and higher surface area, which result in higher dye loadings and better short-circuit current densities than DSCs based on alkaline TiO_2-processed films. On the other hand, the product of charge collection and separation quantum yields in films with TiO_2 obtained by alkaline hydrolysis is c.a. 27% higher than for the acid TiO_2 films. The combination of acid and alkaline TiO_2 nanoparticles as mesoporous layer in DSCs results in a synergic effect with overall efficiencies up to 6.3%, which is better than the results found for devices employing one of the nanoparticles separately. These distinct nanoparticles can be also combined by using the layer-by-layer technique (LbL) to prepare compact TiO_2 films applied before the mesoporous layer. DSCs employing photoanodes with 30 TiO_2 bilayers have shown efficiencies up to 12% higher than the nontreated photoanode ones. These results can be conveniently used to develop optimized synthetic procedures of TiO_2 nanoparticles for several dye-sensitized solar cell applications.

1. Introduction

Dye-sensitized solar cells (DSCs) are one of the new photovoltaic technologies capable of directly and efficiently converting solar light to electrical current at reasonable costs [1–6]. Inspired on natural photosynthesis, sensitization of wide bang-gap semiconductors by selected dyes allows the separation of light harvesting and electron transport functions, which reduces the necessity of high-purity materials to reach reasonable conversion efficiencies [7–9].

Among oxide semiconductors, titanium dioxide, TiO_2, is by far the most commonly used semiconductor in DSCs. It is an inert, nontoxic, cheap, and readily available material with wide band gap (E_{bg} = 3.2 eV) and high refractive index, which are very suitable properties for solar cell applications [10–12]. Several studies have shown that the methodology and the experimental conditions to prepare TiO_2 nanoparticles influence their morphologic and electronic properties and, consequently, the overall performance of DSCs [13–21].

Hore and coworkers [17] reported the influence of hydrolysis pH of titanium(IV) isopropoxide on the interfacial electron transfer kinetics of TiO_2 thin films sensitized by Ru(II) polypyridyl complexes. Their results showed that DSCs with TiO_2 nanoparticles synthesized under alkaline conditions exhibit slower interfacial recombination losses and higher open-circuit voltages than solar cells with oxide particles prepared by acid peptization.

In this paper, we provide new insights on the influence of the hydrolysis pH on the overall efficiency of DSCs, based on morphological characterization of TiO_2 nanoparticles synthesized under acid or alkaline conditions. Bare and sensitized TiO_2 films were analyzed by N_2 adsorption-desorption isotherms, scanning electron microscopy (SEM), and X-ray photoelectron spectroscopy

(XPS). Photoelectrochemical parameters determined for DSCs with nanoparticles obtained in different conditions were rationalized based on their morphological characterization. Additionally, the influence of $TiCl_4$ after treatment on mesoporous oxide surface is investigated, as well as the characteristics of DSCs using, simultaneously, acid and alkaline TiO_2 nanoparticles.

2. Experimental

All chemicals were used as received with the exception of 3-methyl-2-oxazolidinone (Aldrich), which was purified by distillation under reduced pressure. The N3 dye, *cis*-$[Ru(dcbH_2)_2(NCS)_2]$, $dcbH_2$ = 4,4′-dicarboxylic acid-2,2′-bipyridine, was synthesized as previously reported [22].

TiO_2 nanoparticles were prepared by the sol-gel method [23] employing acid or alkaline hydrolysis conditions. In acid route, 12 mL of titanium(IV) isopropoxide (Strem, 98%) was slowly added to 70 mL of 0.1 mol L^{-1} HNO_3 aqueous solution under vigorous stirring. In alkaline hydrolysis, the same volume of titanium(IV) isopropoxide was slowly dropped into 70 mL of 0.1 mol L^{-1} ammonia solution. Both, acid and alkaline, mixtures were left under stirring and heating (80°C) for 8 hours. Aliquots of the resulted sols, named acid and alkaline TiO_2, respectively, were used for deposition of layer-by-layer (LbL) compact films. The remaining aliquots were autoclaved for 8 hours at 200°C in a nonstirred titanium pressure vessel (Parr, 4750 Series), concentrated to ~200 mg mL^{-1}, and stabilized with Carbowax 20 M (Supelco) to yield a paste employed for mesoporous TiO_2 layer.

TiO_2 compact films, used as blocking and contact layers, were deposited onto cleaned FTO substrates (Pilkington, TEC-15, 15 Ω per square) using the LbL technique, as described elsewhere [24]. The substrate was immersed alternately for 5 min in a 10 mg mL^{-1} suspension of the nonautoclaved acid TiO_2 at pH 2 and in a 10 mg mL^{-1} suspension of the nonautoclaved alkaline TiO_2 at pH 8. In this approach, acid and alkaline TiO_2 nanoparticles were used as cations and anions, respectively.

Mesoporous TiO_2 films were deposited directly over FTO substrates or on the compact film by the painting technique [23]. The films were dried at room temperature and sintered at 450°C for 30 minutes. The sensitization was achieved by immersion of electrodes in an N3 saturated ethanolic solution, and the amount of adsorbed dye was determined spectrophotometrically by desorption with NaOH 10^{-4} mol L^{-1} aqueous solution. The surfaces of some TiO_2 films were treated by 0.05 mol L^{-1} $TiCl_4$ solution prior to sensitization, as described elsewhere [25]. Sintered electrodes were immersed into the solution and kept at 70°C for 30 minutes. After treatment, they were washed with water and resintered at 450°C for 30 minutes.

Dye-sensitized solar cells with 0.25 cm^2 active area were assembled in a sandwich-type arrangement [23] using the sensitized TiO_2 photoanode and a transparent Pt-covered FTO as a counterelectrode. A solution of 0.05 mol L^{-1} I_2/0.5 mol L^{-1} LiI/0.5 mol L^{-1} pyridine in 90 : 10 mixture of acetonitrile (Aldrich) and 3-methyl-2-oxazolidinone was used as an electrolyte mediator.

UV-Vis absorption spectra were obtained by using an 8453 UV-Vis spectrophotometer (Hewlett Packard). The size of TiO_2 nanoparticles and the morphology of the films were evaluated by field-emission scanning electron microscopy (FESEM) using a JSM 7401F (JEOL) microscope. Morphological parameters such as surface area and porosity were obtained by using nitrogen adsorption-desorption data acquired in an NOVA 2200e surface area analyzer (Quantachrome Instruments). The data were modeled by the Brunauer-Emmett-Teller (BET) equation [26]. XPS analyses of TiO_2 films were carried out in an ESCALAB 220ixL spectrometer (VG Scientific) equipped with a hemispherical electron energy analyzer using Mg-Kα radiation ($h\nu$ = 1487 eV). Photoelectron spectra were recorded in constant analyzer energy (CAE) mode. The binding energies were measured in reference to the C-1s peak at 284.6 eV.

Photoelectrochemical characterization of DSCs was carried out by current-potential measurements using a PAR 270 galvanostat/potentiostat (EG&G Instruments) system at simulated AM 1.5 solar radiation (100 mW cm^{-2}) provided by a solar simulator (Newport/Oriel), as previously described [24, 27]. Photocurrent action spectra were obtained by using an Oriel system comprised by a 400 W Xe lamp coupled to a 0.25 m Czerny-Turner monochromator as described earlier [28]. All parameters were determined from the average values measured with at least three individual cells of each type of photoanode.

3. Results and Discussion

3.1. Characterization of TiO_2 Nanoparticles. TiO_2 nanoparticles synthesized by acid and alkaline routes were analyzed by N_2 adsorption-desorption isotherms using the BET method. The main morphological parameters are shown in Table 1.

TiO_2 nanoparticles obtained by acid route showed a larger surface area and slightly higher porosity than the ones obtained at alkaline medium. In fact, acid pH hydrolysis results in a very transparent sol, different from the film obtained by alkaline route, which is opaque due to the presence of larger particles and aggregates. Scanning electron micrographs of TiO_2 films deposited over FTO substrates confirm that the alkaline route yields larger nanoparticles, Figure 1. Similar effect was reported by Barbé et al. by changing the pH of hydrothermal treatment of nanoparticles produced after an acid hydrolysis [13].

Typically, acid or alkaline-promoted hydrolysis of Ti(IV) alkoxides occurs as follows [29–31]:

$$(RO)_3\text{–Ti–OR} + H_2O \xrightarrow{OH^- \text{ or } H^+} (RO)_3\text{–Ti–OH} + HO\text{–R} \quad (1)$$

Hydrolysis is followed by a condensation step to yield Ti–O–Ti chains as follows:

$$2(RO)_3\text{–Ti–OH} \longrightarrow (RO)_3\text{–Ti–O–Ti–}(OR)_3 + H_2O \quad (2)$$

Table 1: Morphological parameters determined by the BET method for TiO_2 nanoparticles synthesized in different hydrolysis conditions.

Hydrolysis condition	Surface area/$m^2\ g^{-1}$	Particle diameter[a]/nm	Porosity/%
Acid	128	12	58
Alkaline	88	17	54

[a]Average diameter considering spherical particles.

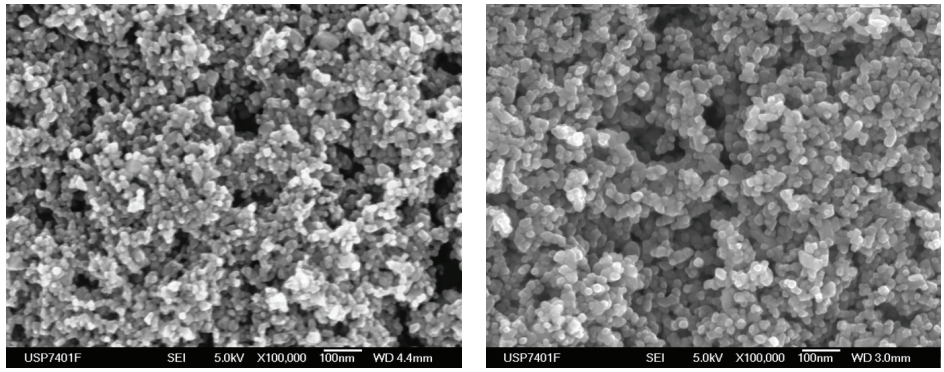

(a) (b)

Figure 1: Scanning electron micrographs of TiO_2 nanoparticles obtained by acid (a) or alkaline (b) routes on FTO.

Continuous hydrolysis/condensation of alkoxyl groups will lead to three-dimensional polymeric Ti–O–Ti chains, which yield TiO_2 particles with different shapes and sizes, depending on experimental conditions (temperature, condensing agents, templates, etc.) [19, 29, 32].

In acid promoted hydrolysis, it is expected that the superficial Ti–OH sites will be constantly protonated during peptization, which decreases the condensation rate and results in smaller particles with positive surface charges that avoid aggregation and increase the porosity of the resulted film. On the other hand, in alkaline catalysis, the superficial Ti–OH $\rightleftharpoons$ Ti–O^- + H^+ equilibrium is shifted to the dissociated form, which facilitates the condensation with other Ti–OH or Ti–OR sites to yield larger nanoparticles. Moreover, during the hydrothermal step in alkaline conditions, the Ostwald ripening effect or coarsening is more effective than in acid medium enhancing the particle growth as discussed by Barbé and coworkers [13]. In the coarsening growth mechanism, larger particles are formed at expense of dissolution of small ones [33]. The growth rate is proportional to the particle solubility and solid-liquid interfacial tension [34]. In alkaline medium, the solubility of TiO_2 is increased, likely due to the complexation of generated anionic species by NH_4^+ ions [13], consequently, the coarsening rate constant is enhanced. The resulted TiO_2 nanoparticles are larger than the particles obtained in acid medium, as can be seen in Figure 1.

Both acidic or alkaline processed, TiO_2 pastes result in 6 to 8 μm thickness films, with considerable different optical properties. The acid TiO_2 films are highly transparent with transmittance of 58% at 500 nm, while the alkaline TiO_2 films exhibit only 40% transmittance at 500 nm.

Adsorption of N3 on both TiO_2 films was carried out in ethanolic solutions without any other reagent. In this condition, the N3 surface concentration on films with nanoparticles obtained by the alkaline pathway (2.6×10^{-8} mol cm^{-2}) is c.a. 3 times lower than that determined for acid TiO_2 nanoparticles (8.6×10^{-8} mol cm^{-2}). Higher surface area as well as concentration of hydroxyl groups on the surface of TiO_2 nanoparticles synthesized under acid conditions justifies higher dye loadings.

XPS analyses of sensitized films have shown similar adsorption modes for both acid and alkaline TiO_2 films. O-1s and Ru-$3d_{5/2}$ signals, Figures 2(a) and 2(b), respectively, are very similar in both films, which indicates that the chemical environments around Ru(II) and O^{2-} ions are the same. In Figure 2(a), one can also observe a broadening of the O-1s peak at the higher binding energy side, which is caused by the presence of free and bounded carboxylate groups from N3 species on TiO_2 surface, as previously discussed [23].

3.2. Photoelectrochemical Behavior of DSCs Employing Acid- or Alkaline-Hydrolyzed TiO_2 Nanoparticles. Photoelectrochemical parameters determined for DSCs prepared with acid or alkaline TiO_2 nanoparticles are shown in Table 2. Some solar cells were prepared with films further treated with $TiCl_4$ solutions in order to increase the quantum yield of charge separation at TiO_2/dye interface, enhancing the photocurrent [25, 35].

One can observe that DSCs prepared with TiO_2 nanoparticles obtained by the acid pathway exhibited conversion efficiencies c.a. 40% higher than the ones using the particles obtained by the alkaline route. Despite their better open-circuit voltages (V_{oc}) and fill factor (ff), the solar cells using alkaline TiO_2 have shown short-circuit current densities (J_{sc}) 50% lower than the acid TiO_2-based DSCs, which is the main reason for the difference observed in the overall efficiency.

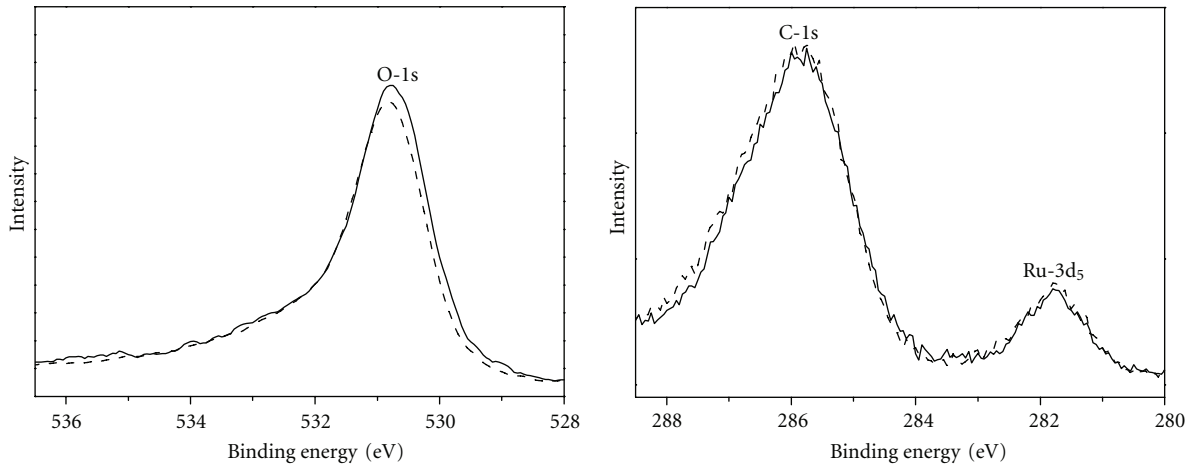

Figure 2: O-1s (a) and Ru-3$d_{5/2}$ (b) peaks of N3-sensitized TiO_2 films prepared by acid (—) or alkaline (- - -) routes.

Table 2: Photoelectrochemical parameters determined for DSCs using TiO_2 obtained by the acid or alkaline routes. (100 mW cm^{-2}, AM 1.5).

Route	V_{oc}/volts	J_{sc}/mA cm^{-2}	ff	η/%
Acid	0.65 ± 0.01	14.0 ± 0.2	0.57 ± 0.03	5.2 ± 0.2
Acid/$TiCl_4$	0.67 ± 0.02	15.0 ± 0.1	0.58 ± 0.02	5.8 ± 0.1
Alkaline	0.71 ± 0.02	8.0 ± 0.3	0.63 ± 0.03	3.6 ± 0.2
Alkaline/$TiCl_4$	0.73 ± 0.01	8.6 ± 0.3	0.66 ± 0.04	4.2 ± 0.2

In DSCs, the short-circuit current (I_{sc}) can be defined by (3) [35], in which I_0 is the incident photon flux in Coulomb s^{-1}, Φ_{lh} is the light-harvesting efficiency, Φ_{cs} is the quantum yield for charge separation at TiO_2/dye interface, and Φ_{col} is the charge collection efficiency. Φ_{lh} is dependent on the nature of the sensitizer and its concentration on the surface, whereas Φ_{cs} and Φ_{col} depend basically on the morphological and electronic properties of the semiconductor metal oxide film

$$I_{sc} = I_0 \Phi_{lh} \Phi_{cs} \Phi_{col}. \quad (3)$$

The reduction of photocurrent observed for the DSCs employing alkaline TiO_2 nanoparticles can be justified by the decrease of Φ_{lh}, since the amount of N3 adsorbed in this film is three times lower than adsorbed on acid TiO_2. In fact, Φ_{lh} is only dependent on the optical and excited state properties of the selected sensitizer. Thus, it can be expected that the observed photocurrent will be proportional to the N3 concentration in each TiO_2 film. However, while the photocurrent of DSCs using the alkaline TiO_2 decreases 40% in relation to the ones using acid TiO_2 films, the N3 concentration in the different photoanodes varies 70%, that is, the photocurrent is not proportional to the N3 concentration.

These results evidence that TiO_2 nanoparticles synthesized under alkaline hydrolysis conditions exhibit better charge separation and charge collection efficiencies. From photoelectrochemical parameters determined in this work, it can be estimated that the product $\Phi_{cs}\Phi_{col}$ is c.a. 27% higher for alkaline TiO_2 in relation to the nanoparticles synthesized in acid conditions. This analysis agrees with previous discussion carried out by Hore and coworkers based on transient absorption data, in which the different dependence of charge recombination rates on applied bias for acid and alkaline TiO_2 films evidences that the alkaline hydrolysis results in a decrease of charge recombination rate [17]. Additional evidence for the better electronic properties of TiO_2 nanoparticles synthesized by alkaline route is given by the lower dark current observed for the DSCs prepared with their films, as in Figure 3.

The surface posttreatment of alkaline TiO_2-based films with acidified $TiCl_4$ solutions resulted in an increase of c.a. 7% of adsorbed N3, similarly to what is observed for acid TiO_2-based films and to earlier reported works [25, 35, 36]. As expected, the photocurrent observed for DSCs with both treated films increases linearly with the N3 concentration, as in Table 2. Photoaction spectra of DSCs show that the $TiCl_4$ treatment improves the light-to-current conversion efficiency in all visible region, as in Figure 4.

Photoanodes comprised by an acid TiO_2 film deposited over an alkaline TiO_2 layer were prepared in an attempt to integrate the better electronic properties of TiO_2 synthesized by the alkaline route with the higher dye loading of the acid-hydrolyzed particles. The resulting solar cells have shown intermediate properties in relation to those with individual acid and alkaline TiO_2 films and, in this new setup, the maximum overall efficiency achieved 6.3%, as shown in Figure 5.

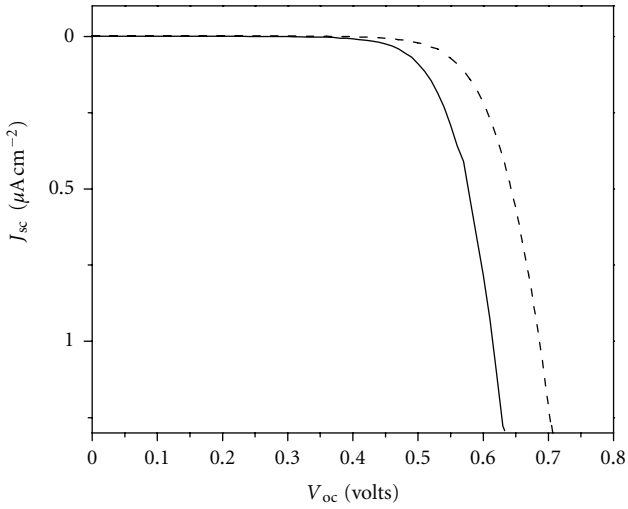

Figure 3: Dark current-voltage curves of DSCs using TiO_2 obtained by the acid (—) or alkaline (- - -) routes.

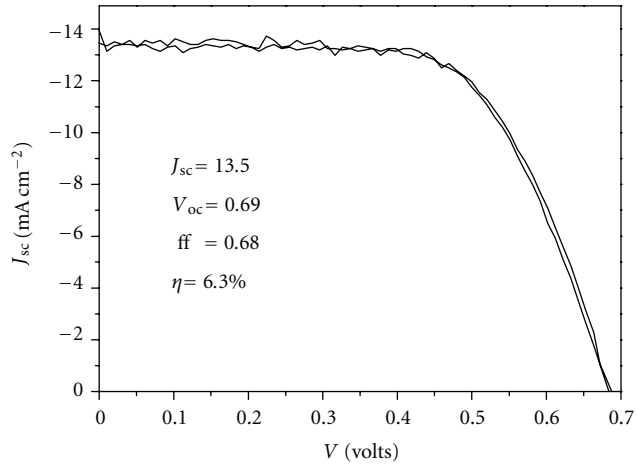

Figure 5: Current-voltage curve for a DSC with a photoanode having an acid TiO_2 film deposited over an alkaline TiO_2 layer (AM 1.5 illumination; 100 mW cm^{-2}).

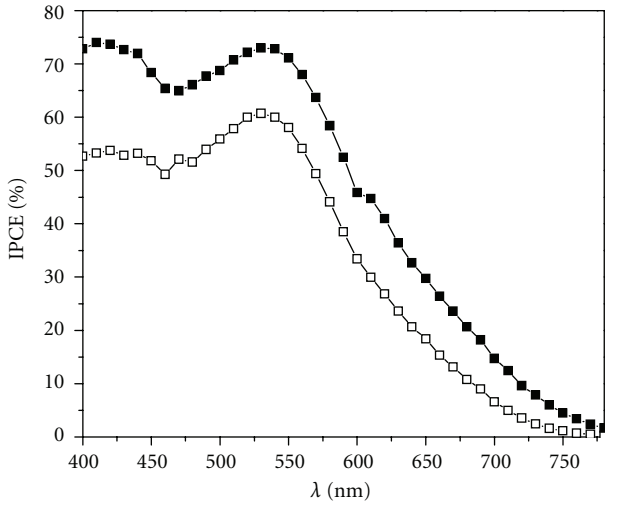

Figure 4: Photocurrent action spectra of DSCs prepared with acid-route TiO_2 films treated (- -■- -) and nontreated (- -□- -) by $TiCl_4$ solutions.

Another effective strategy is the use of a compact oxide layer on the FTO surface beneath the mesoporous semiconductor layer to aggregate the desired morphological and electronic properties of the distinct TiO_2 nanoparticles. Positive charged nonautoclaved acid TiO_2 are attracted by negative charged alkaline ones to yield a compact film over FTO. This procedure leads to self-assembled TiO_2 films more stable to the sintering temperature than those obtained using organic polyanions [37]. Thus, the produced films address the two main requisites to be an efficient compact blocking layer in DSCs [37]: low porosity and temperature stability. This compact film is an elegant solution to prevent the physical contact between the electrolyte and the FTO surface, decreasing the charge recombination at this interface and, consequently, improving the conversion efficiency [38–40].

A mesoporous layer of acid TiO_2 was deposited over the FTO substrate modified by 15 or 30 bilayers of the LbL TiO_2 compact film. The use of resulted electrodes as photoanodes in DSCs increases the solar cell overall efficiency by 6% and 12%, respectively. Thus, the compact film produced with acid and alkaline TiO_2 nanoparticles effectively avoids the charge recombination at FTO/electrolyte interface and improves the electrical contact of FTO with the mesoporous TiO_2 layer [24, 37]. However, these compact films have also led to a decrease of 16% and 23%, respectively, on the transmittance of the FTO substrate. Therefore, when photoelectrochemical data are corrected, the increase on the overall efficiency is, respectively, 26% and 46%.

4. Conclusions

In this work, the influence of pH during hydrolysis of titanium(IV) isopropoxide on the morphologic and electronic properties of TiO_2 thin films is discussed and correlated to the solar light-to-current conversion efficiency of DSCs based on such films. TiO_2 particles hydrolyzed under alkaline conditions exhibit higher diameters, lower porosity, and lower dye loading than the nanoparticles synthesized by the acid route. On the other hand, when N3-sensitized thin films based on alkaline TiO_2 are applied as photoanode in DSCs, one can observe a better charge separation as well as higher charge collection efficiencies, which evidence that electron transport among alkaline TiO_2 nanoparticles is more efficient than in acid TiO_2-based films.

Based on these experimental observations, two new strategies were proposed in order to improve the DSC efficiency. In a first attempt, DSCs were prepared with a photoanode comprised by acid TiO_2 nanoparticles over an alkaline TiO_2-based film, and higher dye loadings are achieved as well as high charge separation and collection efficiencies, which result in a better overall conversion efficiency than DSCs using the nanoparticles separately.

This synergic effect is also achieved in compact layers prepared by the LbL technique using acid TiO_2 as cations and alkaline TiO_2 as anions before the mesoporous layer. The resulted compact film physically prevents the electron recombination at FTO/electrolyte interface and also improves the electrical contact between the conductive substrate and the mesoporous layer. Such a strategy has resulted in an improvement of 12% in the conversion efficiency of solar cells.

Acknowledgments

The authors thank the Fundação de Amparo à Pesquisa do Estado de São Paulo (FAPESP) and the Conselho Nacional de Desenvolvimento Científico e Tecnológico (CNPq) for the financial support. Fundação de Amparo à Pesquisa do Estado de Minas Gerais (FAPEMIG) is acknowledged for supporting XPS analyses. They also thank Pilkington Glass Company for supplying FTO glasses.

References

[1] S. Caramori, V. Cristino, R. Boaretto, R. Argazzi, C. A. Bignozzi, and A. Di Carlo, "New components for dye-sensitized Solar Cells," *International Journal of Photoenergy*, vol. 2010, Article ID 458614, 16 pages, 2010.

[2] A. O. T. Patrocínio, S. K. Mizoguchi, L. G. Paterno, C. G. Garcia, and N. Y. M. Iha, "Efficient and low cost devices for solar energy conversion: efficiency and stability of some natural-dye-sensitized solar cells," *Synthetic Metals*, vol. 159, no. 21-22, pp. 2342–2344, 2009.

[3] N. Y. Murakami Iha, C. G. Garcia, and C. A. Bignozzi, "Dye-sensitized photoelectrochemical cells," in *Handbook of Photochemistry and Photobiology*, H. S. Nalwa, Ed., pp. 49–75, American Scientific Publishers, Stevenson Ranch, Calif, USA, 2003.

[4] M. Grätzel, "Recent advances in sensitized mesoscopic solar cells," *Accounts of Chemical Research*, vol. 42, no. 11, pp. 1788–1798, 2009.

[5] L. M. Goncalves, V. De Zea Bermudez, H. A. Ribeiro, and A. M. Mendes, "Dye-sensitized solar cells: a safe bet for the future," *Energy and Environmental Science*, vol. 1, no. 6, pp. 655–667, 2008.

[6] C. G. Garcia, N. Y. Murakami Iha, R. Argazzi, and C. A. Bignozzi, "Sensitization of *n*-type TiO_2 electrode by a novel isoquinoline ruthenium(II) polypyridyl complex," *Journal of the Brazilian Chemical Society*, vol. 9, no. 1, pp. 13–15, 1998.

[7] C. G. Garcia and N. Y. M. Iha, "Photoelectrochemical solar cells using $[(dcbH_2)_2\ RuLLM']$, L,L′ = substituted pyridines, as nanocrystalline TiO 2 sensitizers," *International Journal of Photoenergy*, vol. 3, no. 3, pp. 130–135, 2001.

[8] A. S. Polo, M. K. Itokazu, and N. Y. Murakami Iha, "Metal complex sensitizers in dye-sensitized solar cells," *Coordination Chemistry Reviews*, vol. 248, no. 13-14, pp. 1343–1361, 2004.

[9] C. G. Garcia, N. Y. Murakami Iha, R. Argazzi, and C. A. Bignozzi, "4-Phenylpyridine as ancillary ligand in ruthenium(II) polypyridyl complexes for sensitization of n-type TiO_2 electrodes," *Journal of Photochemistry and Photobiology A*, vol. 115, no. 3, pp. 239–242, 1998.

[10] H. Tributsch, A. Barkschat, T. Moehl, and B. MacHt, "The function of TiO_2 with respect to sensitizer stability in nanocrystalline dye solar cells," *International Journal of Photoenergy*, vol. 2008, Article ID 814951, 2008.

[11] B. O. Aduda, P. Ravirajan, K. L. Choy, and J. Nelson, "Effect of morphology on electron drift mobility in porous TiO_2," *International Journal of Photoenergy*, vol. 6, no. 3, pp. 141–147, 2004.

[12] K. Kalyanasundaram and M. Grätzel, "Applications of functionalized transition metal complexes in photonic and optoelectronic devices," *Coordination Chemistry Reviews*, vol. 177, no. 1, pp. 347–414, 1998.

[13] C. J. Barbé, F. Arendse, P. Comte et al., "Nanocrystalline titanium oxide electrodes for photovoltaic applications," *Journal of the American Ceramic Society*, vol. 80, no. 12, pp. 3157–3171, 1997.

[14] A. Zaban, S. T. Aruna, S. Tirosh, B. A. Gregg, and Y. Mastai, "The effect of the preparation condition of TiO_2 colloids on their surface structures," *Journal of Physical Chemistry B*, vol. 104, no. 17, pp. 4130–4133, 2000.

[15] F. Lenzmann, J. Krueger, S. Burnside et al., "Surface photovoltage spectroscopy of dye-sensitized solar cells with TiO_2, Nb_2O_5, and $SrTiO_3$ nanocrystalline photoanodes: indication for electron injection from higher excited dye states," *Journal of Physical Chemistry B*, vol. 105, no. 27, pp. 6347–6352, 2001.

[16] S. Kambe, S. Nakade, Y. Wada, T. Kitamura, and S. Yanagida, "Effects of crystal structure, size, shape and surface structural differences on photo-induced electron transport in TiO_2 mesoporous electrodes," *Journal of Materials Chemistry*, vol. 12, no. 3, pp. 723–728, 2002.

[17] S. Hore, E. Palomares, H. Smit et al., "Acid versus base peptization of mesoporous nanocrystalline TiO_2 films: functional studies in dye sensitized solar cells," *Journal of Materials Chemistry*, vol. 15, no. 3, pp. 412–418, 2005.

[18] W. Chen, X. Sun, Q. Cai, D. Weng, and H. Li, "Facile synthesis of thick ordered mesoporous TiO_2 film for dye-sensitized solar cell use," *Electrochemistry Communications*, vol. 9, no. 3, pp. 382–385, 2007.

[19] Y. Mao, T. J. Park, F. Zhang, H. Zhou, and S. S. Wong, "Environmentally friendly methodologies of nanostructure synthesis," *Small*, vol. 3, no. 7, pp. 1122–1139, 2007.

[20] S. Ito, M. K. Nazeeruddin, S. M. Zakeeruddin et al., "Study of dye-sensitized solar cells by scanning electron micrograph observation and thickness optimization of porous TiO_2 electrodes," *International Journal of Photoenergy*, vol. 2009, Article ID 517609, 8 pages, 2009.

[21] D. F. Watson and G. J. Meyer, "Cation effects in nanocrystalline solar cells," *Coordination Chemistry Reviews*, vol. 248, no. 13-14, pp. 1391–1406, 2004.

[22] M. K. Nazeeruddin, A. Kay, I. Rodicio et al., "Conversion of light to electricity by cis-X_2bis(2,2′-bipyridyl-4,4′-dicarboxylate)ruthenium(II) charge-transfer sensitizers (X = Cl-, Br-, I-, CN-, and SCN-) on nanocrystalline TiO_2 electrodes," *Journal of the American Chemical Society*, vol. 115, no. 14, pp. 6382–6390, 1993.

[23] A. O. T. Patrocínio, E. B. Paniago, R. M. Paniago, and N. Y. M. Iha, "XPS characterization of sensitized *n*-TiO_2 thin films for dye-sensitized solar cell applications," *Applied Surface Science*, vol. 254, no. 6, pp. 1874–1879, 2008.

[24] A. O. T. Patrocínio, L. G. Paterno, and N. Y. Murakami Iha, "Layer-by-layer TiO_2 films as efficient blocking layers in dye-sensitized solar cells," *Journal of Photochemistry and Photobiology A*, vol. 205, no. 1, pp. 23–27, 2009.

[25] P. M. Sommeling, B. C. O'Regan, R. R. Haswell et al., "Influence of a $TiCl_4$ post-treatment on nanocrystalline TiO_2 films

in dye-sensitized solar cells," *Journal of Physical Chemistry B*, vol. 110, no. 39, pp. 19191–19197, 2006.

[26] S. Brunauer, P. H. Emmett, and E. Teller, "Adsorption of gases in multimolecular layers," *Journal of the American Chemical Society*, vol. 60, no. 2, pp. 309–319, 1938.

[27] C. G. Garcia, A. S. Polo, and N. Y. Murakami Iha, "Photoelectrochemical solar cell using extract of Eugenia jambolana Lam as a natural sensitizer," *Anais da Academia Brasileira de Ciencias*, vol. 75, no. 2, pp. 163–165, 2003.

[28] A. S. Polo and N. Y. Murakami Iha, "Blue sensitizers for solar cells: natural dyes from Calafate and Jaboticaba," *Solar Energy Materials and Solar Cells*, vol. 90, no. 13, pp. 1936–1944, 2006.

[29] X. Chen and S. S. Mao, "Titanium dioxide nanomaterials: synthesis, properties, modifications and applications," *Chemical Reviews*, vol. 107, no. 7, pp. 2891–2959, 2007.

[30] X. Chen and S. S. Mao, "Synthesis of titanium dioxide (TiO_2) nanomaterials," *Journal of Nanoscience and Nanotechnology*, vol. 6, no. 4, pp. 906–925, 2006.

[31] U. Diebold, "The surface science of titanium dioxide," *Surface Science Reports*, vol. 48, no. 5–8, pp. 53–229, 2003.

[32] P. Pookmanee and S. Phanichphant, "Titanium dioxide powder prepared by a sol-gel method," *Journal of Ceramic Processing Research*, vol. 10, no. 2, pp. 167–170, 2009.

[33] S. L. Isley and R. L. Penn, "Titanium dioxide nanoparticles: effect of sol-gel pH on phase composition, particle size, and particle growth mechanism," *Journal of Physical Chemistry C*, vol. 112, no. 12, pp. 4469–4474, 2008.

[34] M. P. Finnegan, H. Zhang, and J. F. Banfield, "Anatase coarsening kinetics under hydrothermal conditions as a function of Ph and temperature," *Chemistry of Materials*, vol. 20, no. 10, pp. 3443–3449, 2008.

[35] B. C. O'Regan, J. R. Durrant, P. M. Sommeling, and N. J. Bakker, "Influence of the $TiCl_4$ treatment on nanocrystalline TiO_2 films in dye-sensitized solar cells—2. Charge density, band edge shifts, and quantification of recombination losses at short circuit," *Journal of Physical Chemistry C*, vol. 111, no. 37, pp. 14001–14010, 2007.

[36] S. Ito, T. N. Murakami, P. Comte et al., "Fabrication of thin film dye sensitized solar cells with solar to electric power conversion efficiency over 10%," *Thin Solid Films*, vol. 516, no. 14, pp. 4613–4619, 2008.

[37] A. O. T. Patrocinio, L. G. Paterno, and N. Y. M. Iha, "Role of polyelectrolyte for layer-by-layer compact TiO_2 films in efficiency enhanced dye-sensitized solar cells," *Journal of Physical Chemistry C*, vol. 114, no. 41, pp. 17954–17959, 2010.

[38] M.-S. Wu, C.-H. Tsai, and T.-C. Wei, "Electrochemical formation of transparent nanostructured TiO_2 film as an effective bifunctional layer for dye-sensitized solar cells," *Chemical Communications*, vol. 47, no. 10, pp. 2871–2873, 2011.

[39] J. Xia, N. Masaki, K. Jiang, and S. Yanagida, "Sputtered Nb_2O_5 as a novel blocking layer at conducting glass/TiO_2 interfaces in dye-sensitized ionic liquid solar cells," *Journal of Physical Chemistry C*, vol. 111, no. 22, pp. 8092–8097, 2007.

[40] P. J. Cameron and L. M. Peter, "Characterization of titanium dioxide blocking layers in dye-sensitized nanocrystalline solar cells," *Journal of Physical Chemistry B*, vol. 107, no. 51, pp. 14394–14400, 2003.